AMERICAN SOCIETY FOR MICROBIOLOGY | Journal of Virology®

VACCINES AND ANTIVIRAL AGENTS

Attenuated Human Parainfluenza Virus Type 1 Expressing Ebola Virus Glycoprotein GP Administered Intranasally Is Immunogenic in African Green Monkeys

Matthias Lingemann,[a,c] Xueqiao Liu,[a] Sonja Surman,[a] Bo Liang,[a] Richard Herbert,[b] Ashley D. Hackenberg,[b] Ursula J. Buchholz,[a] Peter L. Collins,[a] Shirin Munir[a]

RNA Viruses Section, Laboratory of Infectious Diseases, National Institute of Allergy and Infectious Diseases, National Institutes of Health, Bethesda, Maryland, USA[a]; Experimental Primate Virology Section, Comparative Medicine Branch, National Institute of Allergy and Infectious Diseases, National Institutes of Health, Poolesville, Maryland, USA[b]; Institut für Mikrobiologie, Technische Universität Braunschweig, Braunschweig, Germany[c]

ABSTRACT The recent 2014-2016 Ebola virus (EBOV) outbreak prompted increased efforts to develop vaccines against EBOV disease. We describe the development and preclinical evaluation of an attenuated recombinant human parainfluenza virus type 1 (rHPIV1) expressing the membrane-anchored form of EBOV glycoprotein GP, as an intranasal (i.n.) EBOV vaccine. GP was codon optimized and expressed either as a full-length protein or as an engineered chimeric form in which its transmembrane and cytoplasmic tail (TMCT) domains were replaced with those of the HPIV1 F protein in an effort to enhance packaging into the vector particle and immunogenicity. GP was inserted either preceding the N gene (pre-N) or between the N and P genes (N-P) of rHPIV1 bearing a stabilized attenuating mutation in the P/C gene ($C^{\Delta 170}$). The constructs grew to high titers and efficiently and stably expressed GP. Viruses were attenuated, replicating at low titers over several days, in the respiratory tract of African green monkeys (AGMs). Two doses of candidates expressing GP from the pre-N position elicited higher GP neutralizing serum antibody titers than the N-P viruses, and unmodified GP induced higher levels than its TMCT counterpart. Unmodified EBOV GP was packaged into the HPIV1 particle, and the TMCT modification did not increase packaging or immunogenicity but rather reduced the stability of GP expression during *in vivo* replication. In conclusion, we identified an attenuated and immunogenic i.n. vaccine candidate expressing GP from the pre-N position. It is expected to be well tolerated in humans and is available for clinical evaluation.

IMPORTANCE EBOV hemorrhagic fever is one of the most lethal viral infections and lacks a licensed vaccine. Contact of fluids from infected individuals, including droplets or aerosols, with mucosal surfaces is an important route of EBOV spread during a natural outbreak, and aerosols also might be exploited for intentional virus spread. Therefore, vaccines that protect against mucosal as well as systemic inoculation are needed. We evaluated a version of human parainfluenza virus type 1 (HPIV1) bearing a stabilized attenuating mutation in the P/C gene ($C^{\Delta 170}$) as an intranasal vaccine vector to express the EBOV glycoprotein GP. We evaluated expression from two different genome positions (pre-N and N-P) and investigated the use of vector packaging signals. African green monkeys immunized with two doses of the vector expressing GP from the pre-N position developed high titers of GP neutralizing serum antibodies. The attenuated vaccine candidate is expected to be safe and immunogenic and is available for clinical development.

KEYWORDS Ebola GP, Ebola glycoprotein GP, vaccine, Ebola virus, human parainfluenza virus, human parainfluenza virus type 1, intranasal vaccine, live attenuated vaccine, mucosal vaccine, vectored vaccine

Received 22 December 2016 **Accepted** 17 February 2017

Accepted manuscript posted online 1 March 2017

Citation Lingemann M, Liu X, Surman S, Liang B, Herbert R, Hackenberg AD, Buchholz UJ, Collins PL, Munir S. 2017. Attenuated human parainfluenza virus type 1 expressing Ebola virus glycoprotein GP administered intranasally is immunogenic in African green monkeys. J Virol 91:e02469-16. https://doi.org/10.1128/JVI.02469-16.

Editor Terence S. Dermody, University of Pittsburgh School of Medicine

Address correspondence to Shirin Munir, munirs@niaid.nih.gov.

Ebola virus (EBOV) is a nonsegmented negative-sense RNA virus that belongs to the family *Filoviridae*, which consists of three genera: *Marburgvirus*, *Ebolavirus*, and *Cuevavirus* (1). EBOV causes severe hemorrhagic fever in humans, with a fatality rate of up to 90% (2). The genus Ebolavirus has five known subtypes: Zaire, Sudan, Bundibugyo, Taï Forest, and Reston. Zaire EBOV, the most pathogenic subtype, caused the 2014-2016 EBOV outbreak in West Africa, the largest outbreak in history, with over 28,000 cases and >11,000 deaths (3). No licensed vaccine or postexposure treatment is presently available, and the unprecedented scale of the recent outbreak raised concerns of further outbreaks and spread.

EBOV can be transmitted by puncture wounds or contact of a patient's body fluids with skin or mucosal surfaces. More recently, aerosol transmission via airborne droplets of body fluids has received increased recognition as an important mode of transmission (4). For example, aerosolized EBOV can cause lethal infection in nonhuman primates (NHPs) and guinea pigs (5) and can be transmitted from infected to naive animals by aerosols (6, 7). Guinea pigs infected with aerosolized EBOV are more infectious for naive animals than those infected intraperitoneally (7). This stresses the need to develop an EBOV vaccine capable of inducing both systemic and mucosal immunity, particularly in the respiratory tract.

The EBOV glycoprotein GP is a highly glycosylated surface antigen that is anchored in the membrane in a type I orientation (i.e., the membrane anchor is near the C terminus). GP mediates viral attachment and entry (8) and is the major neutralization antigen. Vectored vaccines expressing GP induce protective immune responses against lethal EBOV challenge in NHPs (9–13). EBOV expresses two major forms of GP: one is a 50- to 70-kDa secreted protein (sGP) encoded by unmodified GP mRNA, and the other is a 120- to 130-kDa transmembrane glycoprotein (GP_0) encoded by a form of the mRNA in which a single A residue (mRNA-sense) has been added at a specific editing site by transcriptional editing. GP_0 represents the primary translation product of the complete GP open reading frame (ORF) and is 676 residues in length. GP_0 is cleaved by a furin-like protease into two subunits, GP_1 and GP_2 (representing, respectively, the N-terminal three-quarters and C-terminal one-quarter of GP_0), that remain linked by a disulfide bond. The vectors in the present study involve expression of GP_0, which hereafter is referred to as GP or full-length GP.

Human parainfluenza virus serotype 1 (HPIV1) is an enveloped, nonsegmented, negative-strand RNA virus of the family *Paramyxoviridae*. The HPIV1 genome consists of 6 genes encoding the nucleoprotein (N), phosphoprotein (P/C), internal matrix protein (M), fusion glycoprotein (F), hemagglutinin-neuraminidase glycoprotein (HN), and the large polymerase protein (L) (14). The P gene carries an additional overlapping open reading frame expressing the C proteins, which antagonize host interferon and apoptosis responses (15). We previously developed a non-temperature-sensitive attenuating mutation, called $C^{\Delta 170}$, that consists of a 6-nucleotide deletion in the overlapping P and C ORFs (16, 17). This mutation reduces the ability of C proteins to inhibit the host type I interferon response and apoptosis (15, 18, 19), resulting in viral attenuation. We previously evaluated HPIV1 as a vaccine vector for expressing the respiratory syncytial virus (RSV) fusion (F) glycoprotein and showed that the HPIV1-$C^{\Delta 170}$ backbone was the better of two attenuated backbones (17).

Human parainfluenza virus serotype 3 (HPIV3) is another member of the *Paramyxoviridae* and shares considerable sequence relatedness and similarities in genome organization with HPIV1 (they are both in the genus *Respirovirus*). We previously evaluated HPIV3 (JS strain) expressing EBOV GP as an intranasal (i.n.) vaccine candidate called rHPIV3/EboGP (9, 20, 21). In NHPs, one i.n. dose was moderately immunogenic, with 88% protection, but two doses provided complete protection against an intraperitoneal EBOV challenge. However, the JS strain has not been specifically attenuated, and it has a potential risk of vector-related respiratory illness (22), especially in children and the elderly; thus, an attenuated vector would be preferable. Also, the comparative properties of the different types of HPIVs as vectors have not been examined, and it is unclear which type would be the most effective as a human vaccine vector.

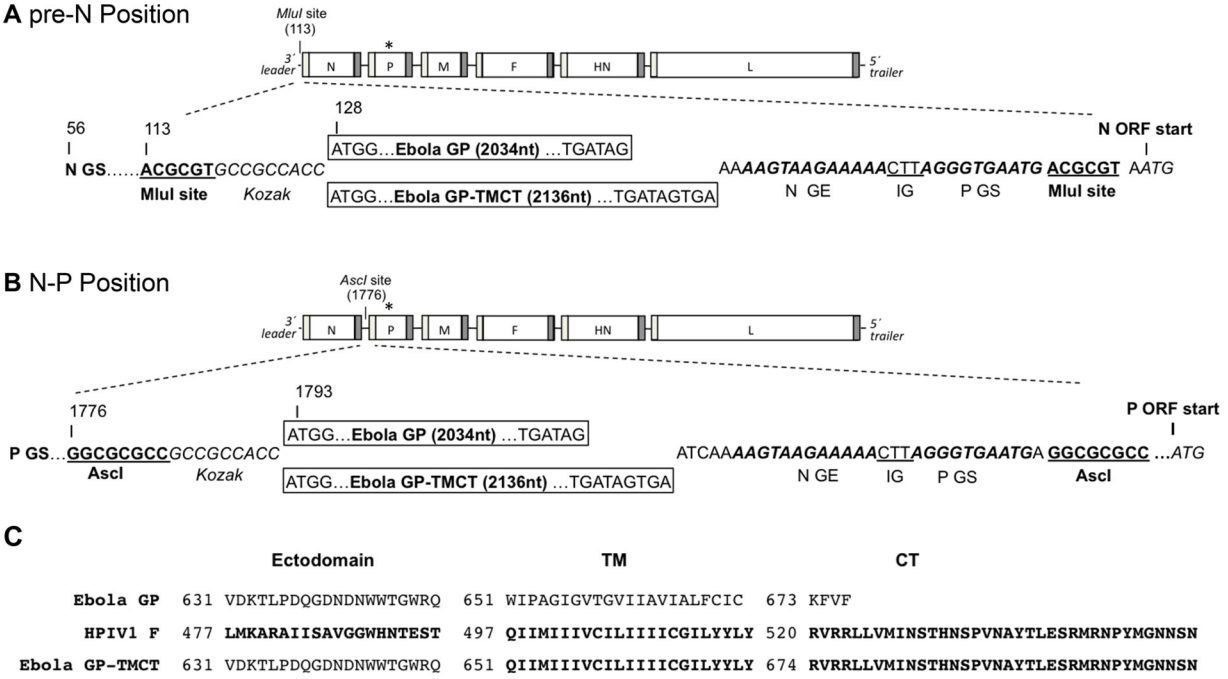

FIG 1 Construction of antigenomic cDNAs of rHPIV1-C$^{\Delta 170}$ expressing full-length EBOV GP or chimeric EBOV GP with HPIV1 F transmembrane (TM) and cytoplasmic tail (CT) domains from the pre-N (A) or N-P (B) position. The EBOV GP ORF (strain Mayinga; GenBank accession number AF086833.2) was modified by the insertion of a single A residue at the editing site so as to encode full-length GP. The ORF was codon optimized and inserted, as either the full-length GP or as a chimeric form in which the TMCT domain was replaced with that of HPIV1 F, at the pre-N (A) or N-P (B) position of rHPIV1-C$^{\Delta 170}$ bearing an attenuating mutation in the P/C ORF (indicated by an asterisk) using the previously introduced (17) unique MluI or AscI restriction sites, respectively. The GP insert was engineered with flanking HPIV1 gene transcription signals to allow for its expression as a separate mRNA. The amino acid alignment of EBOV GP, HPIV1 F, and the chimeric EBOV GP-TMCT, where the TM and CT of EBOV GP has been replaced with that of HPIV1 F (bold), is shown in panel C.

In a recent study, we demonstrated that incorporation of RSV F protein in a PIV3 vector particle was substantially enhanced by replacing its transmembrane and cytoplasmic (TMCT) domains with those of the vector F protein (23). The TMCT modification resulted in a significant increase in both the quantity and quality of serum antibodies against vector-expressed RSV F protein. This likely reflects increased immunogenicity of an antigen presented to the immune system in a particle, and it also may reflect increased immunogenicity of antigen presented in a native, ordered array (24). Similar results have been obtained using HPIV1-based vectors expressing the RSV F protein (unpublished data). This indicates that for HPIV3 and HPIV1 vectors, incorporation of a heterologous glycoprotein into the vector particle increases its immunogenicity. In this regard, it is noteworthy that we previously showed that the incorporation of EBOV GP into the HPIV3 vector particle was only 13% as efficient as the HPIV3 HN protein, suggestive of inefficient packaging of EBOV GP into an HPIV vector (21).

In the present study, we developed rHPIV1-C$^{\Delta 170}$ vectors expressing EBOV GP from the pre-N (first position; 3′ proximal of the N gene) or N-P (second position; between N and P genes) positions (Fig. 1). Two sites were chosen to determine the effect of the GP insert position on HPIV1 attenuation, GP expression, and immunogenicity. At each site, EBOV GP was expressed either as the full-length unmodified GP protein or as a derivative of GP in which the TMCT domains were swapped for those of the HPIV1 F protein in an effort to achieve efficient incorporation into the vector particle (Fig. 1). The viruses were analyzed for *in vitro* growth and GP and vector protein expression, followed by evaluation in NHPs for replication, GP stability, and immunogenicity. This study identified a promising vaccine candidate for clinical development.

RESULTS

Recovery of the rHPIV1-C$^{\Delta 170}$ vectors expressing EBOV GP. Recombinant HPIV1 (rHPIV1) bearing the attenuating Δ170 mutation in the C gene was modified by reverse

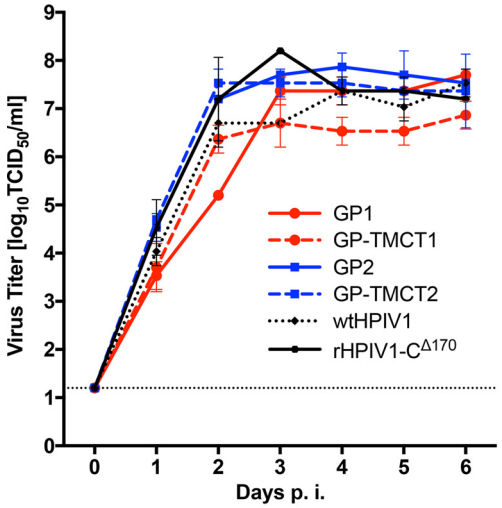

Virus[a]	1	2	3	4	5	6
GP1	**	****	*	ns	ns	ns
GP-TMCT1	*	*	****	*	*	ns
GP2	ns	ns	ns	ns	ns	ns
GP-TMCT2	ns	ns	ns	ns	ns	ns

[a] Mean titers compared to the rHPIV1-C$^{\Delta 170}$ empty backbone: ns, not significant; *, P < 0.05; **, P < 0.01; ****, P < 0.0001

FIG 2 Multistep growth kinetics. Vero cells were infected in triplicate with an MOI of 0.01 $TCID_{50}$/cell with each indicated HPIV1-C$^{\Delta 170}$ virus expressing EBOV GP or GP-TMCT virus. The cells were incubated at 32°C, and aliquots of culture supernatant were collected at 24-h intervals over 6 days. Virus titers were determined by limiting dilution on LLC-MK2 cells using a hemadsorption assay. Titers are reported as log_{10} $TCID_{50}$ per milliliter. Mean titers are shown, with the standard deviations as vertical error bars. The statistical significance of the difference between EBOV GP viruses (GP1, GP-TMCT1, GP2, and GP-TMCT2) and the rHPIV1-C$^{\Delta 170}$ empty backbone was determined by two-way analysis of variance with Tukey's multiple-comparison posttest and is shown in the table below the graph.

genetics to express the GP ORF that was modified by the insertion of an additional A residue (mRNA-sense) at the gene editing site, which mimics EBOV-specific editing and creates a frameshift to encode the full-length 676-amino-acid membrane-anchored GP. The ORF also was codon optimized for human expression. In addition, a second version was made in which this ORF was modified further to replace its TMCT domain with that of the HPIV1 F protein (Fig. 1C) in an effort to enhance incorporation into the rHPIV1 vector particle. The ORF encoding GP or GP-TMCT was inserted in the pre-N (Fig. 1A) or the N-P (Fig. 1B) position of HPIV1 as an added gene under the control of HPIV1 GS and GE transcription signals. The constructs containing the GP or GP-TMCT insert in the pre-N position were called GP1 and GP-TMCT1, and those with GP or GP-TMCT in the N-P position were called GP2 and GP-TMCT2. All constructs were readily recovered, and after an additional single passage on LLC-MK2 cells, the viral genome sequences were determined and were found to be free of adventitious mutations.

Multicycle growth kinetics. The ability of vaccine candidates to efficiently replicate *in vitro*, critical for vaccine manufacture, was assessed by determining their multistep growth kinetics on Vero cells, which is the cell substrate for vaccine manufacture (Fig. 2). Wild-type (wt) HPIV1 and rHPIV1-C$^{\Delta 170}$ were included as the parental controls. The viruses generally were similar in growth kinetics and final titers, with peak titers between 6.5 and 8.0 log_{10} 50% tissue culture infective doses ($TCID_{50}$)/ml. The GP1 virus had a significantly lower titer on day 2, suggestive of reduced growth kinetics, but reached a peak titer on day 3 similar to that of rHPIV1 C$^{\Delta 170}$. GP-TMCT1 was significantly attenuated compared to the empty backbone on day 1 to 5 but reached a final peak titer on day 6 which was similar to those of other viruses.

Stability of GP expression in virus stocks. To determine the plaque phenotype and the stability of expression of GP and GP-TMCT, we monitored expression by a

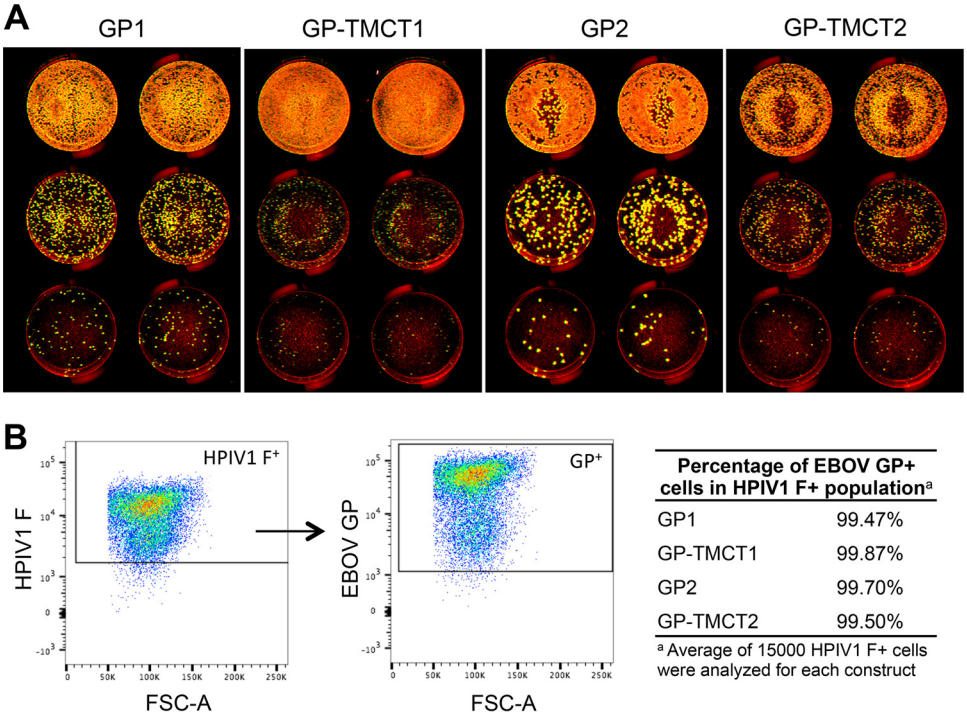

Percentage of EBOV GP+ cells in HPIV1 F+ population[a]	
GP1	99.47%
GP-TMCT1	99.87%
GP2	99.70%
GP-TMCT2	99.50%

[a] Average of 15000 HPIV1 F+ cells were analyzed for each construct

FIG 3 Stability of EBOV GP expression by HPIV1 vectors. (A) Double-staining plaque assay. Vero cells were inoculated with a 10-fold serial dilution of each virus in duplicate, and infected monolayers were incubated for 6 days at 32°C under 0.8% methylcellulose overlay. Immunostaining was performed with mouse monoclonal anti-EBOV GP and goat polyclonal anti-HPIV1 antibodies. Secondary antibodies included infrared dye-labeled donkey anti-mouse 800CW and donkey anti-goat 680LT. Plaque images were acquired with an Odyssey infrared imaging system, and the percentage of plaques expressing EBOV GP was determined. The infrared dyes were pseudocolored to appear red and green for HPIV1 and EBOV GP, respectively. On merging the colors, the plaques coexpressing GP and HPIV1 antigens appeared yellow and those not expressing GP were red. Representative monolayers are shown as examples. (B) Double-staining flow cytometry assay. Vero cells infected with the vectors were stained with anti-HPIV1 F and anti-EBOV GP (KZ52) monoclonal antibodies as described in Materials and Methods and analyzed on a BD FACSCanto II. An example of EBOV GP staining of HPIV1 F^+ single live cells is shown as scatter plots, and the stability of EBOV GP expression (percentage of EBOV GP^+ cells in HPIV1 F^+ population) for all vectors is shown as a table.

dual-staining immunoassay using primary antibodies specific to GP and HPIV1 proteins and differentiating secondary antibodies tagged with infrared fluorescent dyes. GP antigen was imaged as red, HPIV1 antigen was imaged as green, and coexpression was imaged as yellow. First, the dual staining was performed in a plaque assay format on Vero cells (Fig. 3A). For all viruses, no plaques were detected that did not express EBOV GP (Fig. 3A), suggesting close to 100% expression. The pre-N viruses had an overall reduced plaque size compared to that of N-P viruses, suggesting that GP insertion in the promoter-proximal position reduced the efficiency of virus replication and/or spread. The plaque size was even further reduced for the GP-TMCT versions compared to their full-length GP counterparts (Fig. 3A), suggesting an attenuating effect of TMCT.

Since the small plaque size of the GP-TMCT viruses made it difficult to clearly assess staining, the dual-staining assay was performed in a flow cytometry format. Vero cells were infected with the various vectors at a multiplicity of infection (MOI) of 5 $TCID_{50}$/cell and incubated at 32°C for 24 h. The cells were stained for HPIV1 F and EBOV GP antigen and analyzed by flow cytometry. For all constructs, >99% of HPIV1 F^+ cells (~15,000 cells analyzed for each construct) also expressed EBOV GP (Fig. 3B). Thus, the plaque assay and flow cytometric analysis showed that all viruses maintained stable expression of EBOV GP or GP-TMCT during *in vitro* replication.

Expression of EBOV GP in infected-cell lysates. To quantify the expression of EBOV GP or GP-TMCT and HPIV1 vector proteins in infected cells, Vero cells were infected with the various vectors at an MOI of 3 $TCID_{50}$/cell and subjected to Western

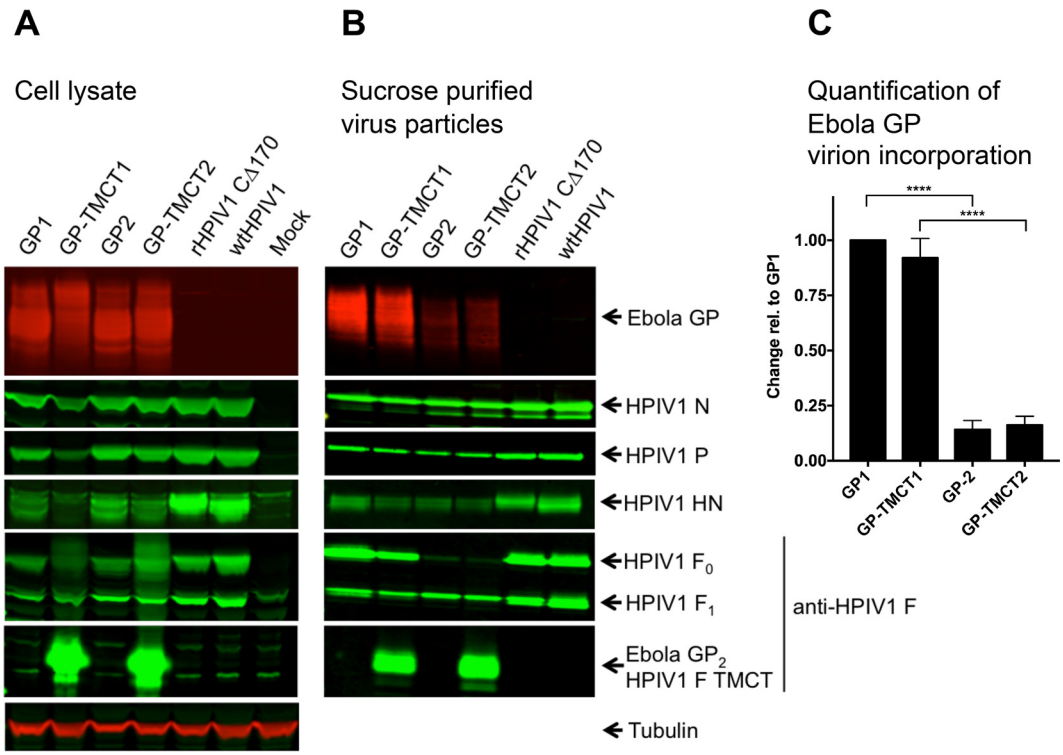

FIG 4 Western blot analysis of infected cell lysates and sucrose gradient-purified virions. (A) Cell lysates. Vero cells were infected at an MOI of 3 $TCID_{50}$/cell with the indicated viruses and incubated for 48 h at 32°C, after which cells were lysed in LDS sample buffer and analyzed by Western blotting. EBOV GP was detected with mouse anti-GP and anti-mouse IRDye 680 RD antibodies. Individual HPIV1 proteins were detected with rabbit polyclonal hyperimmune sera raised individually against peptides derived from HPIV1 N, P, F, and HN proteins, as previously described (17). Tubulin was detected on all blots, as a loading control, using mouse antitubulin and anti-mouse IRDye 680RD antibodies; a representative blot is shown. (B) Sucrose-purified virus particles. LLC-MK2 cells were infected at an MOI of 0.1 $TCID_{50}$ per cell with the indicated viruses and incubated for 6 days at 32°C, and virus particles were purified by sucrose step gradient centrifugation. For each virus, 1 μg of total protein, measured by BCA assay, was analyzed by Western blotting using the same antibodies as described above. (C) Relative quantification of EBOV GP incorporation into HPIV1 virions. EBOV GP signals on the blots were quantified (Licor-Image Studio) for three independent experiments and normalized to HPIV1 P, which was detected simultaneously on each blot. Quantification is shown relative to GP packaged in GP1 particles (set at a value of 1.0). The statistical significance of the differences in the amount of virion-packaged GP was determined by one-way analysis of variance with Tukey's multiple-comparison posttest and is indicated by four asterisks ($P < 0.0001$).

blot analysis at 48 h postinfection (p.i.). All constructs expressed a considerable amount of GP/GP-TMCT. Note that for the Western blot analysis, gel electrophoresis was performed under reducing conditions (which would dissociate G_1 and G_2), and the GP-specific monoclonal antibody used in the analysis recognizes full-length GP_0 and GP_1 but not GP_2. Because full-length GP_0 and GP_1 are close in molecular weight, the wide GP band detected in the Western blot analysis in Fig. 4 might include either or both of the full-length GP_0 and GP_1 forms. This detail is immaterial to the results.

HPIV1 has a polar gradient of gene expression, with the greatest expression for 3′ proximal genes compared to downstream genes. Thus, a gene inserted closer to the 3′ end would be expected to express more protein than from a downstream location. However, the gradient effect was not evident in this study: specifically, the levels of GP and GP-TMCT expression from the pre-N and N-P positions were similar (Fig. 4A). In contrast, expression of the vector genes was consistent with the expected gradient effect: specifically, viruses bearing a GP or GP-TMCT insert showed reduced expression of downstream vector proteins compared to those of wt HPIV1 and HPIV1 $C^{\Delta 170}$ empty vector. This reduction was somewhat greater for the pre-N than for the N-P viruses. This reduction also was greater with GP-TMCT versions than for their respective GP constructs. This last effect likely was not an effect of the transcriptional gradient, since the number and arrangement of genes were not affected by the TMCT swaps. Thus, the insert position (i.e., pre-N versus N-P) appeared to have little or no effect on GP or

GP-TMCT expression (however, see Discussion), but it did reduce vector protein expression.

Incorporation of EBOV GP into the rHPIV1 vector particle. The purpose of making the EBOV GP-TMCT versions (GP-TMCT1 and GP-TMCT2) was to have the TMCT domain of GP be HPIV1 specific and thus compatible with the HPIV1 virion proteins, such as the M protein, that are involved in virion morphogenesis. This might increase the efficiency of EBOV GP incorporation into the vector particles and might also affect its arrangement on the surface of the particles. To assess the efficiency of packaging, each virus was propagated in LLC-MK2 cells for 7 days and partially purified by sedimentation through discontinuous sucrose gradients. Purified virus was lysed, and 1 μg of total protein of each was analyzed by Western blotting.

GP and GP-TMCT appeared to be efficiently incorporated into the HPIV1 virions when expressed from the pre-N gene position (Fig. 4B, GP1 and GP-TMCT1). Surprisingly, the TMCT modification did not appear to further enhance GP incorporation (GP1 versus GP-TMCT1). The efficiency of packaging was significantly reduced when GP and GP-TMCT were expressed from the N-P gene position (GP2 and GP-TMCT2): specifically, the amount of GP and GP-TMCT packaged for the pre-N viruses was on average 6.3-fold larger than that of N-P viruses (Fig. 4C). This was calculated relative to the HPIV1 P protein, whose efficiencies of packaging were similar for all four of the GP- and GP-TMCT-expressing vectors.

Expression of the GP and GP-TMCT inserts had effects on the efficiency of virion incorporation of the vector proteins, compared to wt HPIV1 and the rHPIV1-C$^{\Delta 170}$ empty vector. For example, viruses expressing GP and GP-TMCT showed dramatic reductions in the incorporation of vector HN, although this effect was somewhat less with GP1. Another difference was that the level of incorporation of HPIV1 F was much lower for the N-P viruses (GP2 and GP-TMCT2), which also had much less GP and GP-TMCT incorporation, as noted above. Incidentally, almost all of the HPIV1 F packaged in the N-P particles was in the cleaved form (F_1), with very little F_0. In contrast, the pre-N viruses (GP1 and GP-TMCT1) had considerably more incorporation of HPIV1 F, as well as GP and GP-TMCT as noted above, and cleavage of HPIV1 F was less complete and resembled that of wt HPIV1. All viruses were propagated, harvested, and purified side by side under similar conditions. The basis for the increased cleavage efficiency for the N-P viruses is not clear.

The antiserum specific to HPIV1 F protein had been raised against a synthetic peptide representing the C-terminal 17 amino acids of the CT of HPIV1 F protein. Therefore, in addition to detecting HPIV1 F_0 and F_1 (Fig. 4B, 5th blot from the top), this antiserum also detected the GP_2 fragment present in the GP-TMCT virions, due to the presence of the CT domain from the HPIV1 F protein (6th blot from the top). The amounts of GP_2 in this blot appear similar for GP-TMCT1 and GP-TMCT2 despite a much larger amount of the former than the latter packaged in the virions as detected with the GP-specific antibody (top blot). This is likely because of a larger amount of uncleaved full-length GP_0 (not shown) in GP-TMCT1 than in GP-TMCT2 virions, and hence, the GP_2 band does not reflect total GP in the particles. This GP_2 fragment was also detected in the infected-cell lysates for GP-TMCT viruses (Fig. 4A, 6th blot from the top). As noted, the GP_2 fragment was not recognized by the GP-specific monoclonal antibody and therefore does not otherwise appear in these blots.

Replication of vaccine candidates in AGMs. The HPIV1-C$^{\Delta 170}$ vectors expressing EBOV GP or GP-TMCT were evaluated in African green monkeys (AGMs). Four animals per group were infected by the combined i.n. and intratracheal (i.t.) routes with 10^6 $TCID_{50}$ per site. As controls, two animals were infected with wt HPIV1 and two additional animals were infected with a previously described candidate, rHPIV3/EboGP, consisting of wt rHPIV3 that expresses EBOV GP from the third gene position (P-M) (21). Nasopharyngeal (NP) swabs (upper respiratory tract [URT]) and tracheal lavage (TL) samples (lower respiratory tract [LRT]) were collected daily and every other day,

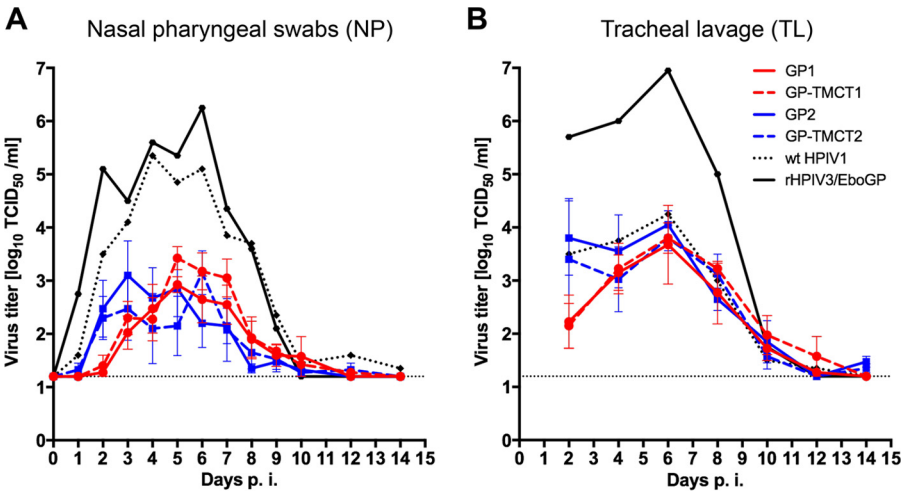

FIG 5 Replication of rHPIV1 expressing EBOV GP in AGMs. Groups of four animals were inoculated with 10^6 $TCID_{50}$ in 1 ml each via the intranasal and intratracheal routes with the indicated HPIV1-$C^{\Delta 170}$ viruses expressing EBOV GP or GP-TMCT. Two animals were inoculated with wt HPIV1 or HPIV3/EboGP. Nasopharyngeal swabs were collected daily (A) and tracheal lavages were performed every other day (B) during the 2 weeks postinoculation. Virus titers were determined by limiting dilution on LLC-MK2 cells and hemadsorption. The average titers are shown as $\log_{10}$ $TCID_{50}$ per milliliter, with the standard errors of means indicated by error bars. Note that values indicate virus titers after the first dose; replication of the booster dose could not be detected and is not shown.

respectively, for 14 days postinfection. Virus shedding was quantified by an infectivity assay and reported as $\log_{10}$ $TCID_{50}$/ml (Fig. 5).

All of the HPIV1-based GP and GP-TMCT constructs were attenuated in the URT and grew to a peak titer of approximately 3 $\log_{10}$ $TCID_{50}$/ml, in contrast to wt HPIV1, which grew to a titer of 5 $\log_{10}$ $TCID_{50}$/ml (Fig. 5A). Viruses with GP or GP-TMCT in the N-P position (GP2 and GP-TMCT2) appeared to replicate somewhat faster in the URT compared to those in the pre-N position (GP1 and GP-TMCT1), although these differences were not statistically significant. Specifically, the N-P viruses were recovered at higher titers during days 1 to 3; by day 4 p.i., the pre-N and N-P viruses reached similar titers; and thereafter, the titers of the pre-N viruses generally were higher. In the LRT, there was little evidence of attenuation of the HPIV1-based GP and GP-TMCT constructs compared to wt HPIV1, and all of these constructs reached peak titers of approximately 4 $\log_{10}$ $TCID_{50}$/ml on day 6 p.i. (Fig. 5B). As in the URT, replication of the N-P constructs was more efficient during the first few days after infection.

In comparison, rHPIV3/EboGP replicated to significantly higher titers than the HPIV1-based vectors, reaching peak titers of 6 and 7 $\log_{10}$ $TCID_{50}$/ml in URT and LRT, respectively. The greater replication of the HPIV3-based candidate was not unexpected, since it employs a fully wt backbone in contrast to the attenuated HPIV1 backbone. In addition, wt HPIV3 was previously shown to replicate in AGMs to titers that were 10- to 30-fold higher than those for wt HPIV1 (25).

At 28 days p.i., two animals per group were boosted by reinfection with the same virus, using the same routes and dose as for the first infection. NP and TL samples were collected during days 1 to 14 p.i., as described for the first infection. Replication of each of the booster doses was undetectable by the infectivity assay (limit of detection $\leq$ 1.2 $\log_{10}$ $TCID_{50}$/ml) in any of the specimens from any of the animals (data not shown), indicating that there was substantial restriction of replication and shedding.

Analysis of EBOV GP-specific serum IgG by ELISA. From the AGM experiment described in the preceding section, serum samples were collected weekly from the immunized animals for evaluation of the EBOV-specific serum antibody response. Sera collected on days 28, 35, and 56 p.i. were subjected to an EBOV GP-specific IgG enzyme-linked immunosorbent assay (ELISA) (Fig. 6). At 28 days p.i. (sera collected just before the booster administration), only modest titers of EBOV GP-specific IgG were

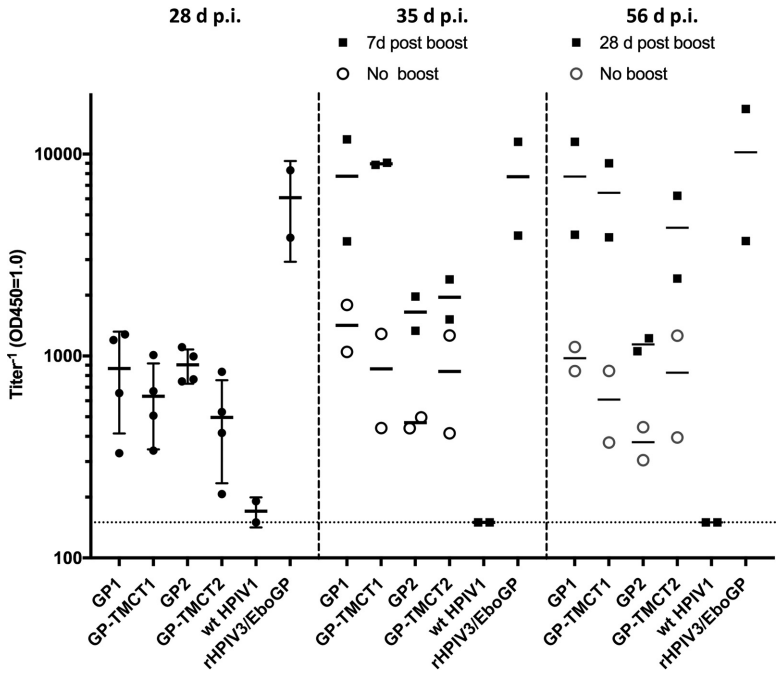

FIG 6 EBOV GP-specific serum IgG titer. Sera of the immunized AGMs collected at 28 days (d), 35 days (7 days postboost), and 56 days (28 days postboost) after the first immunization were analyzed by an EBOV-GP capture ELISA specific for IgG. Titers for individual animals are shown by symbols. Open circles indicate animals that did not receive the booster dose on day 28. Horizontal bars indicate mean titers; for day 28 p.i., standard deviations are shown as error bars. Values are reported as reciprocal titers of an OD_{450} of 1.0.

detected for any of the HPIV1-based constructs. However, at day 35 (day 7 postboost), those animals that had received a booster dose of GP1 or GP-TMCT1 vectors showed a 10-fold increase in antibody titers, reaching levels similar to those of rHPIV3/EboGP. These titers did not increase further (i.e., at day 56, or 28 days postboost). No detectable differences were observed between the GP1 and GP-TMCT1 titers. In the case of AGMs immunized with GP2 or GP-TMCT2, there was only a modest increase in titer at day 35, and there was a further modest increase by day 56 only in the case of GP-TMCT2.

In contrast, the primary immunization with unattenuated rHPIV3/EboGP induced high IgG titers detected at 28 days, but the subsequent boost showed only a minimal effect at days 35 and 56. In comparison, two doses of the attenuated rHPIV1-based vectors, particularly those expressing GP1 and GP-TMCT1, conferred titers of EBOV GP-specific IgG that were similar to those of rHPIV3/EboGP, and this was observed as early as 7 days postboost.

Analysis of EBOV-neutralizing serum antibody responses. A 60% plaque reduction neutralization test ($PRNT_{60}$) was developed to evaluate the ability of serum antibodies from the AGM study to bind and neutralize virus bearing EBOV GP. To obviate a biosafety level 4 (BSL4) facility, we constructed (not shown) a recombinant HPIV3 called rHPIV3/NotI ΔF-HN/EboGP, in which the HPIV3 HN and F genes were replaced by a gene encoding EBOV GP so that EBOV GP was the sole viral envelope glycoprotein available to mediate attachment and entry. This virus was very similar to one that we previously described (20). Although slightly attenuated compared to wt HPIV3, this virus is capable of efficiently infecting cells, grows to high titers (~7.5 $\log_{10}$ PFU/ml), and forms distinct plaques under methylcellulose overlay, indicating that EBOV GP in the virion particles is functional and likely retains the neutralization epitopes.

We confirmed the specificity of the neutralization assay using several control antibodies. First, we showed that the construct was strongly neutralized by the EBOV GP-specific antibody KZ52, which is a human monoclonal IgG from an EBOV survivor

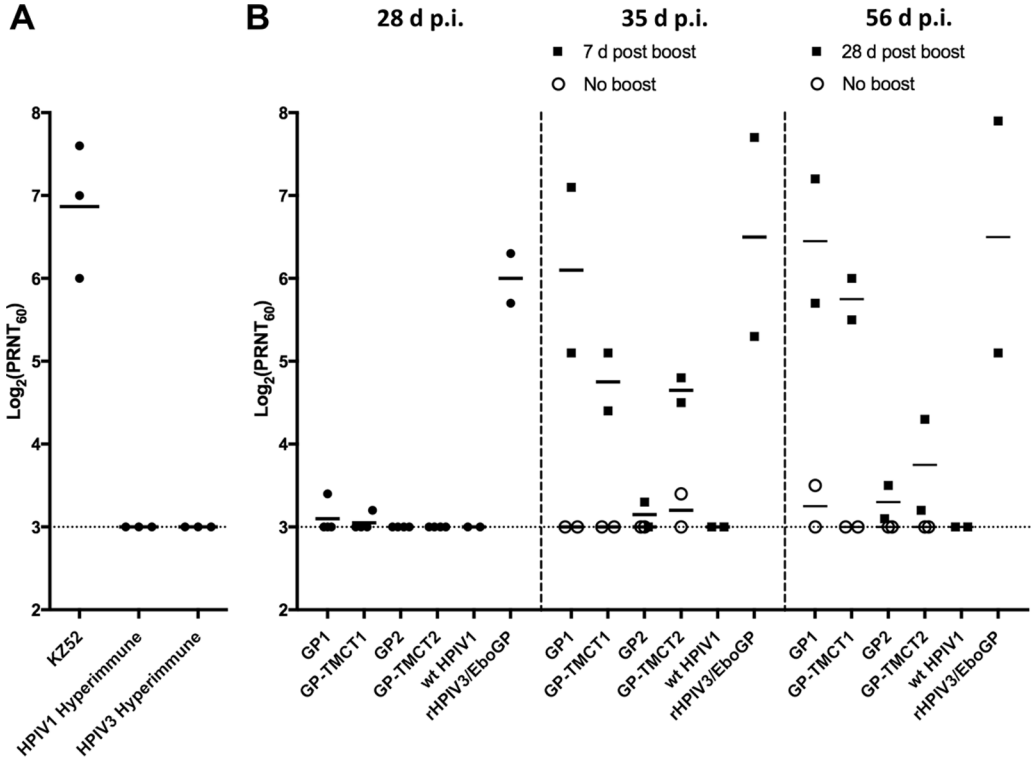

FIG 7 EBOV GP-specific 60% plaque reduction neutralization assay. Serum samples were analyzed for 60% plaque reduction neutralization test ($PRNT_{60}$) titer using rHPIV3/NotI ΔF-HN/EboGP virus. (A) KZ52, a human monoclonal EBOV GP antibody known to have GP neutralizing activity, was used as a positive control. Rabbit hyperimmune sera against HPIV1 and HPIV3 were included as controls to determine any neutralizing activity of HPIV1- or HPIV3-specific antibodies for rHPIV3/NotI ΔF-HN/EboGP. (B) Sera from the immunized African green monkeys at 28 days, 35 days (7 days postboost), and 56 days (28 days postboost) after the first immunization were analyzed by virus neutralization assay, and the $PRNT_{60}$ titers were determined for rHPIV3/NotI ΔF-HN/EboGP in the presence of guinea pig complement. Open circles indicate animals that did not receive a booster on day 28 after primary immunization. The average $PRNT_{60}$ titer for each group is shown with the horizontal bars.

(Fig. 7A). Second, we investigated whether the construct was sensitive to neutralizing polyclonal antisera specific to HPIV1 or HPIV3. Possible neutralization by HPIV3-specific antisera was important to investigate because of the presence in the rHPIV3/NotI ΔF-HN/EboGP construct of all of the HPIV3 proteins except F and HN. Possible neutralization by HPIV1-specific serum was important to investigate because HPIV1 and HPIV3 belong to the same genus (*Respirovirus*) and share substantial sequence relatedness, although they are considered distinct serotypes. We therefore performed the neutralization assay with a hyperimmune rabbit antiserum raised against HPIV3 (which had a $PRNT_{60}$ titer against HPIV3 of >13 $\log_2$) and a second hyperimmune rabbit antiserum raised against HPIV1 (which had a $PRNT_{60}$ titer against HPIV1 of 7.3 $\log_2$). Neither antiserum had detectable neutralizing activity against rHPIV3/NotI ΔF-HN/EboGP (Fig. 7A). Thus, any neutralization activity by the AGM sera should be due to EBOV-specific antibodies.

At 28 days p.i. no significant serum neutralization activity could be detected for any of the rHPIV1-GP constructs. In comparison, the rHPIV3/EboGP control induced a $PRNT_{60}$ titer of approximately 6.0 $\log_2$. However, the animals that had received a second dose of the GP1 virus reached neutralization titers nearly as high as those of animals that had received a second dose of rHPIV3/EboGP, and this was observed as early as 7 days postboost. GP-TMCT1 and GP-TMCT2 did show an increase in antibody titers, but these were lower than those of GP1. Animals that had not received a second dose showed undetectable (limit of detection by $PRNT_{60}$: 3 $\log_2$) or very low neutralizing activity. The virus neutralization titers closely reflected the ELISA results and showed that within 7 days postboost the GP1 vaccine candidate conferred neutralizing

TABLE 1 Percentage of HPIV1-C$^{\Delta 170}$-GP plaques expressing EBOV GP after replication in African green monkeys, determined by a double-staining plaque assay[a]

		% of plaques positive for EBOV GP					
		Nasopharyngeal swabs			Tracheal lavage		
Virus	Monkey ID	P1	P2	P3	P1	P2	P3
GP1	7856	98	100	97	90	67 (3)	100 (5)
	8054	65	75	70 (10)	81	94	100
	7867	95	87	92	100	98	98
	8172	99	99	97	100	97	99
GP-TMCT1	8445	56	52	71	100	96	100 (9)
	8195	33	41	47	86	89	79
	8392	75	36	47	92	91	99
	8258	50	19	15	83	67 (6)	93
GP2	8555	67 (3)	50 (8)	33 (3)	97	100	100
	8401	90	100	100 (4)	100	96	94
	62403	98	92	98	100	97	100
	8246	100 (2)	99	100	99	98	95
GP-TMCT2	8577	ND	50 (6)	100	91	84	95
	8573	23	91	14 (7)	100	98	100
	57413	0 (10)	60 (5)	ND	67 (3)	100	100 (4)
	8232	74	56	66	97	96	91

[a]Vero cell monolayers were infected with serially diluted samples of NP and TL specimens from the indicated animals (from the experiment shown in Fig. 5; ID, identifier), incubated for 6 days under a methylcellulose overlay, fixed, and subjected to immunostaining against EBOV GP (green) and HPIV1 (red). Plaques that stained for both appeared yellow; plaques in which expression of GP was lost appeared red. The percentage of plaques positive for expression of EBOV GP was the number of yellow plaques divided by the total number of plaques (red and yellow). P1 is the day before peak shedding, P2 is the day of peak shedding, and P3 is the day after peak shedding for that particular animal. For samples with ≤10 plaques, the total numbers of plaques are shown in parentheses. Underlined values represent samples also shown in Fig. 8. ND, not determined because titers of samples were below the limit of detection.

titers comparable to those of rHPIV3/EboGP, which has been previously shown to protect NHPs against EBOV challenge (21). Although GP-TMCT1 induced ELISA IgG titers similar to those of GP1, its neutralizing titers were slightly lower. Similar to the case with ELISA, the virus neutralizing titers also did not substantially increase between 7 and 28 days postboost, suggesting that the maximum attainable titers were achieved within a week after the boost.

Stability of EBOV GP expression during replication in AGMs. The stability of EBOV GP expression during replication in AGMs was evaluated by a double-staining plaque assay. For the four animals in each of the GP1, GP-TMCT1, GP2, and GP-TMCT2 groups in the experiment in Fig. 5, we analyzed NP and TL samples from the day of peak shedding for each particular animal (designated P2) as well as for the preceding day (P1) and the following day (P3). The samples were analyzed by the double-staining plaque assay, and the percentage of HPIV1 plaques coexpressing EBOV GP was determined (Table 1). Representative images of plaques of each construct are shown (Fig. 8).

Overall, the candidates expressing EBOV GP from either the pre-N or N-P position (GP1 and GP2) had a more stable GP expression than their TMCT counterparts (GP-TMCT1 and GP-TMCT2). In the case of GP1, 3 of 4 animals (numbers 7856, 7867, and 8172) showed an average stability of 95% in both NP and TL samples, and the remaining animal (number 8054) was 70% stable in NP samples but was more stable, at 92%, in TL samples. GP-TMCT1 was substantially less stable in the NP samples, with an average of 45% plaques expressing GP, whereas the TL samples were more stable, at 90%. Similar to GP1, in the case of the GP2-immunized group, 3 of 4 animals (numbers 8401, 62403, and 8246) had an average stability of 97% in both NP and TL samples, while the remaining animal (number 8555) had 50% GP expression in NP but 99% in TL samples. Similar to the case with GP-TMCT1, a tendency of reduced stability was observed for GP-TMCT2, with averages of 53% and 93% expression in NP and TL

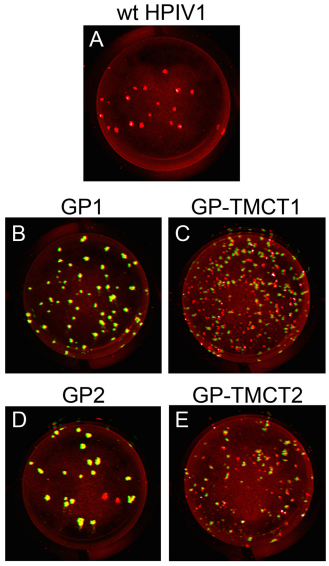

FIG 8 Representative results of the double-staining plaque assay used to determine the stability of EBOV GP expression during replication in African green monkeys. Representative examples of double-stained Vero monolayers are shown from the experiment in Table 1 (see Table 1 for details). (A) wt HPIV1, animal 32956, TL, day P2; (B) GP1, animal 7856, NP, day P1; (C) GP-TMCT1, animal 8392, NP, day P3; (D) GP2, animal 62403, NP, P2; (E) GP-TMCT2, animal 8232, NP, day P2. Vero cells were infected with serially diluted NP or TL samples, incubated for 6 days under a methylcellulose overlay, fixed, and subjected to immunostaining against EBOV GP (green) and HPIV1 (red). A representative plate is shown for each indicated specimen. Plaques that stained for both HPIV1 and EBOV GP appeared yellow; plaques in which expression of EBOV GP was lost appeared red. P2 is the day of peak shedding for that particular animal, P1 is the day before the peak of shedding, and P3 is the day following peak shedding. The complete experiment is summarized in Table 1.

samples, respectively. Although the TMCT modification did not increase GP incorporation in the particles and had no evidence of instability during *in vitro* growth, it seems to strongly encourage *in vivo* selection of virus progeny with silenced GP expression.

DISCUSSION

Respiratory tract immunization with a live-attenuated vector offers several advantages over parenteral administration. In addition to inducing systemic immunity, i.n. vaccines induce a mucosal antibody response and respiratory tract resident $CD4^+$ and $CD8^+$ T cells (10), which would be expected to protect against EBOV infection via aerosol, skin, or mucosal routes. Intranasal vaccination is needle free and thus eliminates the concern for spreading blood-borne pathogens in the areas where EBOV is endemic.

The goal of this study was to develop an i.n. vaccine against EBOV based on an attenuated HPIV1-$C^{\Delta 170}$ backbone expressing EBOV GP. One aspect of this study was to increase safety by using an attenuated virus instead of a wt virus as was previously used in rHPIV3/EboGP. The $C^{\Delta 170}$ mutation in HPIV1 was designed in previous studies to confer stability against deattenuation and to confer substantial attenuation in NHPs (15), and it thus should have increased safety in humans. Another aspect of this study was to explore the possibility of increasing GP immunogenicity by increasing its packaging in the vector particle by TMCT modification. As noted (see the introduction), we previously observed that efficient incorporation of the RSV F protein into PIV vectors increased the quantity and quality of the antibody response against the heterologous protein (23). Since the incorporation of EBOV GP into an HPIV3 vector particle in a previous study was only 13% as efficient as that of the HPIV3 HN protein (21), increased efficiency of packaging would be desirable. Therefore, we replaced the GP TMCT domain with that of HPIV1 F in an attempt to increase GP packaging and immunogenicity. A third aspect of this study was to evaluate two different insertion sites for EBOV GP, namely, the pre-N position, which places the GP gene in the first, promoter-

proximal position, and the N-P position. The GP gene was modified to represent an "edited" transcript expressing the GP_0 protein. We also evaluated the effect of a boost.

A total of four different constructs were developed to represent combinations of the two main variables: (i) insertion into the pre-N versus N-P site, and (ii) the presence or absence of the TMCT modification. All four constructs were recovered successfully by reverse genetics. Each of the viruses replicated efficiently in Vero cells and reached a final titer similar to that of wt HPIV1. There was some evidence of modest attenuating effects due to the EBOV GP insert. For example, the two pre-N viruses showed a delay in replication kinetics *in vitro*, with the TMCT version being slower of the two. Also, both of the TMCT constructs had a reduction in plaque size, indicating a slight reduction in replication or spread.

Since the EBOV GP gene is an added gene that is not essential for vector replication, it had the potential to readily accept mutations that might silence its expression. This was monitored by double-straining plaque assay and flow cytometry that assessed expression of EBOV GP by each HPIV1 plaque and infected cell, respectively. Each of the four constructs maintained stable EBOV GP expression during replication in Vero cells. In contrast, all four HPIV1-GP constructs exhibited instability of EBOV GP expression during replication in AGMs, determined by the double-staining assay. The TMCT versions exhibited greater instability than did the GP1 and GP2 versions. It may be that the TMCT substitution in EBOV GP was somewhat inhibitory to vector replication (consistent with the smaller plaque sizes for the TMCT constructs noted above), perhaps due to intracellular competition with TMCT present in HPIV1 F protein. In addition, loss of GP expression was more frequent for all four constructs in the NP versus TL specimens. This may reflect a greater selective pressure in the URT than in the LRT to silence GP expression. We note that the HPIV1-GP constructs were substantially more attenuated than wt HPIV1 in the URT, whereas there was little difference in the LRT. If this attenuation was due, at least in part, to expression of the GP insert, then mutations that silence expression of GP could provide a selective advantage. This is reminiscent of observations with a PIV vector expressing the RSV F protein, which also acquired mutations that would silence expression of the foreign gene (26). However, if silencing the expression of EBOV GP did provide a selective advantage, that advantage may not be very great, because there was not a progressive increase with time in the loss of GP expression during AGM infection. In any event, expression of EBOV GP by the GP1 and GP2 constructs had a high level of stability.

The magnitudes of EBOV GP expression in infected Vero cells were analyzed by Western blotting and were found to be similar for all four constructs at 48 h p.i. This similarity in expression between the pre-N and N-P positions suggests that the expected polar gradient in transcription was not observed, which also is consistent with our previous findings for RSV F protein expressed from HPIV1 (17). In contrast, Western blot analysis of sucrose-purified virions did show a gradient effect, with 6.3-fold more EBOV GP incorporated in the pre-N versus N-P viruses (Fig. 4B and C). This contrast between the GP profile in infected-cell lysates and purified virus may reflect differences in kinetics and timing of accumulation. Specifically, the cell lysates represent protein accumulation during 48 h, and since the kinetics of *in vitro* replication of the pre-N viruses lagged behind that of the N-P viruses during the initial days of infection, that may have counterbalanced an increased expression from the pre-N position. In contrast, the virus particles were purified after 7 days of propagation, and under these conditions the replication of the pre-N constructs would catch up with that of the N-P constructs, and increased expression from the pre-N position could become evident. Another important observation was that EBOV GP was readily detected in virions for each of the constructs, as also had been observed in a previous study with HPIV3 (21), and that the amount of GP in virions of GP-TMCT1 and GP-TMCT2 was similar to that in GP1 and GP2, respectively. This indicates that the TMCT modification did not increase the incorporation of EBOV GP into the HPIV1 vector particles.

In AGMs, the four constructs replicated over several days to peak titers of approximately 3.0 $\log_{10}$ $TCID_{50}$/ml in the URT and 4.0 $\log_{10}$ $TCID_{50}$/ml in the LRT. Compared

to wt HPIV1, the four constructs were attenuated approximately 100-fold in the URT but did not appear to be attenuated in the LRT. The HPIV1-based constructs replicated to titers that were ~1,000-fold lower than rHPIV3/EboGP, a difference that reflected (i) the presence of an attenuating mutation in the HPIV1 constructs but not the HPIV3 construct and (ii) a greater permissiveness of AGMs for HPIV3 versus HPIV1 (25). When a booster dose (of constructs based on HPIV1-$C^{\Delta 170}$ or HPIV3) was given at 28 days after first immunization, there was no detectable shedding of infectious virus. This indicates that the first dose of either vector (HPIV1-$C^{\Delta 170}$ or HPIV3) was sufficiently immunogenic to strongly restrict replication of the booster dose. This restriction would be due to immunity induced against the HPIV1 vector but also might involve immunity induced against the expressed EBOV GP, since this is present in the vector particle.

Measurement of the serum antibody response to EBOV GP by a GP-specific, IgG-specific ELISA showed that by 28 days p.i., all four HPIV1-GP constructs had induced only modest titers of EBOV GP-specific IgG titer. In comparison, HPIV3/EboGP induced a higher titer of EBOV GP-specific IgG, likely reflecting its much higher (1,000-fold) replication in AGMs than that of the attenuated HPIV1-$C^{\Delta 170}$. At 28 days, two animals per group received a booster dose, while two remained unboosted for comparison. Despite the lack of booster virus shedding, evaluation of serum samples taken 7 days following the boost revealed 5.5- and 10.4-fold increases in IgG titers for GP1 and GP-TMCT1, respectively, which reached titers similar to those of rHPIV3/EboGP. These titers did not further increase between 7 and 28 days postboost, indicating that maximum titers had already been attained. The N-P constructs also showed a slight increase in IgG titers after boost, but the magnitude was lower than those of the pre-N viruses, which might possibly be explained by the larger amount of EBOV GP incorporated into the virions at the pre-N than at the N-P position. The rapid increase of IgG titers by 7 days postboost suggests that while the first dose did not induce a robust response by day 28, it did prime for an anamnestic response to the booster dose. Thus, two doses of HPIV1 constructs were necessary but sufficient to boost the EBOV GP-specific antibodies to titers comparable to those of rHPIV3/EboGP.

The EBOV-neutralizing serum antibody response was measured using a $PRNT_{60}$ based on the rHPIV3/NotI ΔF-HN/EboGP construct, from which the surface HPIV3 F and HN proteins had been deleted and replaced by EBOV GP as the sole viral surface glycoprotein. Antibodies to GP, but not HPIV1 or HPIV3, neutralized this virus, validating this assay for measuring GP-specific neutralizing serum antibodies in the AGM specimens. This obviated BSL4 containment. The $PRNT_{60}$ titers correlated with the ELISA titers and showed a similar relative profile. At 28 days p.i., only rHPIV3/EboGP had induced detectable neutralization activity. At 7 days postboost, the $PRNT_{60}$ titers of GP1-vaccinated animals increased to titers similar to those of rHPIV3/EboGP, which have been shown to protect NHPs against EBOV challenge (21). Although GP-TMCT1 had ELISA IgG titers similar to those of GP1 at 7 days postboost, its neutralizing titers were lower, suggesting a loss of neutralizing epitopes by the TMCT modification. Interestingly, despite the delayed replication of pre-N viruses in AGMs, their antibody titers were higher than those of the N-P viruses, possibly reflecting an overall larger amount of GP incorporated in the virions (Fig. 4B). Although animals in each group showed similar tendencies, no statistical analyses were possible due to the limited animal number.

The observation that the second dose of the HPIV1-based constructs did not result in shedding detectable by an infectivity assay, yet resulted in substantial antibody boosts, is reminiscent of previous findings with the rHPIV3/EboGP vector (27). In that study, inoculation of HPIV3-experienced rhesus monkeys with two doses of rHPIV3/EboGP vector given at an interval of 28 days did not result in any shedding detectable by an infectivity assay, yet each dose induced an increase in GP-specific antibodies. In that study, further analysis of the NP and TL specimens by quantitative reverse transcription-PCR (RT-PCR) showed that in fact viral RNA was shed following each dose in HPIV3-experienced animals, probably in the form of virus that was neutralized by antibodies present in the respiratory secretions. The ability of HPIV1 and HPIV3 to

reinfect virus-experienced hosts is not unexpected, since reinfection by these viruses is common in humans. The ability of HPIV1 and HPIV3 to reinfect virus-experienced hosts sufficiently well to be immunogenic suggests that they can be successfully used as vectors in the general population.

The finding that TMCT modification of EBOV GP did not increase incorporation of GP into the vector particle, and did not increase antibody responses to GP, was incongruous to our previous findings with RSV F. One possible explanation is that for whatever reason, EBOV GP already is packaged to the limit of its capacity in the HPIV1 particle, although the previous HPIV3 study indicated that this is substantially lower on a relative molar basis than for the vector HN surface glycoprotein. Another possible explanation is that replacement of the TMCT of EBOV GP (which includes a short CT domain, containing only four amino acids [KFVF]) with the TMCT of the HPIV1 F protein (which has a CT of 36 residues) had the effect of destabilizing GP structure and antigenicity. It has also been previously reported that changes in the TMCT region of EBOV GP affect its functionality (28). This is also supported by the evidence that despite several attempts, we could not rescue an HPIV3/ΔF-HN virus (surface F and HN deleted) expressing a chimeric EBOV GP in which either the CT or the TMCT domain was replaced with that of HPIV3 F protein (unpublished data), whereas rHPIV3/NotI ΔF-HN/EboGP expressing native GP was readily rescued. This suggested that replacement of the CT and TMCT rendered GP nonfunctional. It also may have caused denaturation of protective epitopes. This also is consistent with the observed slight attenuation and microplaque phenotype of the TMCT versions compared to the case with full-length GP (Fig. 3), which suggests that the TMCT form may be nonfunctional and even a disadvantage for the vector.

Overall, the results of this study showed that two doses of the attenuated HPIV1-$C^{\Delta 170}$-based GP1 construct were capable of stimulating high GP neutralizing antibody titers that were similar in magnitude to those induced by the previously described wt HPIV3-based rHPIV3/EboGP construct, which was shown to protect against EBOV challenge (21). However, the HPIV1 vector in the present study has the advantage of bearing a mutation in the P/C gene that confers restricted replication and attenuation needed for safety. In addition, the fact that HPIV1 naturally is less permissive for replication in AGMs than HPIV3 means that the immunogenicity of the HPIV1-based constructs probably is substantially underestimated in this animal model. Specifically, it is possible that two doses would not be needed in the more permissive human host. In addition, the HPIV1-based vaccine could be administered as an aerosol using a nebulizer, which primes the respiratory tract more robustly and may enhance immunogenicity, as was previously shown for rHPIV3/EboGP (10). In conclusion, this study identified the HPIV1-$C^{\Delta 170}$-based GP1 construct as an immunogenic and promising i.n. EBOV vaccine candidate expected to be well tolerated in humans.

MATERIALS AND METHODS

Viruses and cells. HPIV1 virus and cDNAs were derived from HPIV1/Washington/20993/1964 (GenBank accession number AF457102). HPIV1 and derivatives were propagated in LLC-MK2 cells in serum-free Opti-MEM I medium (Life Technologies, Grand Island, NY) containing 1.2% trypsin (TrypLE Select; Life Technologies), 100 U/ml of penicillin, 100 μg/ml of streptomycin (Life Technologies), and 1 mM L-glutamine. HPIV1 titers were determined by 10-fold serial dilution in 96-well plates of LLC-MK2 cells in the same medium and incubation at 32°C with 5% CO_2 for 7 days. Infected cells were detected by hemadsorption (HAD) assay using guinea pig erythrocytes, and titers were calculated as the $\log_{10}$ 50% tissue culture infective dose ($TCID_{50}$) per milliliter. HPIV3 viruses were propagated in LLC-MK2 cells in the same medium as described for HPIV1 except that it contained 5% fetal bovine serum (FBS; Thermo Scientific, Atlanta, GA) instead of trypsin (29). LLC-MK2 cells (ATCC CCL-7) and Vero cells (ATCC CCL-81) were maintained in Opti-MEM I medium with GlutaMax-I (Life Technologies) supplemented with 5% FBS. BHK BSR-T7/5 cells that constitutively express T7 RNA polymerase (30) were maintained in Glasgow's minimal essential medium (MEM; Life Technologies) supplemented with 10% FBS, 1× MEM amino acid solution (Life Technologies), and 1× Geneticin (Life Technologies). Geneticin was included in the medium at every other passage.

Construction of HPIV1 viruses expressing GP or GP-TMCT. The EBOV GP nucleotide sequence used was that of the EBOV Mayinga strain isolated in 1976 (GenBank accession number AF086833.2) (31), which is identical to the other candidate vaccines under evaluation (11, 13). Unedited GP mRNA contains a stretch of 7 A's at the editing site and is translated as secreted GP. Transcriptional editing results in the

addition of a nontemplate A residue at this site, causing frameshift and translation of full-length membrane-anchored GP (8). For our constructs, an edited GP gene containing 8 U residues (negative sense) at the editing site (nucleotide [nt] position 880 to 887, transcribing to 8 A's in the GP mRNA) was used to synthesize membrane-anchored GP. The editing site was previously shown to be unstable in HPIV3 and was stabilized by 2 silent changes to AAGAAGAA (21). For the present study, the GP nucleotide sequence was codon optimized for human expression (Genscript, Piscataway, NJ) with the exception of the AAGAAGAA sequence, which was left undisturbed. In addition, a derivative of GP was made in which the TMCT region was deleted and replaced with the TMCT region of HPIV1 F (Fig. 1C), which was presumptively identified based on hydrophobicity analysis.

We inserted the coding sequence for EBOV GP or EBOV GP-TMCT into the first (pre-N) or second (N-P) gene position of cDNA encoding rHPIV1-C$^{\Delta 170}$ (Fig. 1). For insertion into the pre-N position, the EBOV GP and GP-TMCT cDNAs were designed to be flanked on the upstream side by an MluI site and on the downstream side by a cassette containing the gene end (GE) signal of the N gene, followed by an intergenic (IG) triplet, the gene start (GS) signal of the P gene, and an MluI site (Fig. 1A). For insertion into the N-P gene position, the EBOV GP and GP-TMCT cDNAs were designed to be flanked on the upstream side by an AscI site and on the downstream side by the N GE, IG, and P GS sequences already noted, followed by an AscI site (Fig. 1B). All viruses were designed to keep the hexameric genome nucleotide length (rule of six) (32). Each vector gene maintained its wild-type hexamer phasing except that the N gene in the pre-N constructs had the P gene phasing. The GP and GP-TMCT inserts in pre-N and N-P sites had the hexamer phasing of the N and P genes, respectively. All inserts were synthetically derived (Genscript) and cloned into the rHPIV1-C$^{\Delta 170}$ antigenomic plasmid containing the unique restriction sites MluI and AscI in the pre-N and N-P positions, respectively, using published methods (17). This resulted in four constructs: the two with inserts in the pre-N position were called GP1 and GP-TMCT1, and the two with inserts in the N-P position were called GP2 and GP-TMCT2.

Recovery of the rHPIV1-C$^{\Delta 170}$ vectors expressing EBOV GP from cDNA. The viruses were rescued by cotransfecting BHK BSR T7/5 cells with each of the full-length antigenomic plasmid and support plasmids expressing the HPIV1 N, P, and L proteins as described previously (33, 34). Transfected cells were incubated overnight at 37°C and washed twice with Opti-MEM I medium. The medium was replaced with fresh Opti-MEM I medium with 1 mM L-glutamine and 1.2% trypsin, followed by incubation at 32°C. At 48 h posttransfection, cells were harvested by scraping into the medium and the cell suspension was added to 50% confluent monolayers of LLC-MK2 cells in Opti-MEM I medium, 1 mM L-glutamine, and 1.2% trypsin (Life Technologies) and incubated at 32°C until cytopathic effects were visible. Recovered virus (seed pool) was amplified by one passage (working pool) in LLC-MK2 cells at 32°C. Virus titers were determined at 32°C by HAD with guinea pig erythrocytes, and titers are reported as $\log_{10}$ $TCID_{50}$ per milliliter.

Viral genome sequencing was performed to confirm that the recovered viruses contained the correct genome sequence. Viral RNA was extracted from the virus stocks using a viral RNA extraction kit (Qiagen, Valencia, CA), including DNase digestion to eliminate any plasmid DNA used for virus recovery. Overlapping fragments of the genome were amplified by RT-PCR using the SuperScript first-strand synthesis system (Life Technologies) and Advantage-HF PCR kit (Clontech, Mountain View, CA), followed by Sanger sequencing of the RT-PCR fragments. All viruses were sequenced in their entirety except for the 26 nt at the 5′ end and 86, 79, 77, and 77 nt at the 3′ end of GP1, GP-TMCT1, GP2, and GP-TMCT2, respectively. All viruses were found to be free of adventitious mutations.

Multicycle replication kinetics. Confluent Vero cells in 6-well plates were infected with the recombinant viruses at an input multiplicity of infection (MOI) of 0.01 $TCID_{50}$/cell in triplicate. At 24-h intervals, starting on day 1 through day 6, 500 μl (one-sixth of the volume) of culture medium supernatant was collected from each well and replaced with fresh medium. The samples were flash frozen and stored at −80°C. The virus titer of each sample was determined in duplicate by HAD assay on LLC-MK2 cells as described above.

Double-staining plaque assay. A double-staining fluorescent plaque assay detecting the coexpression of HPIV1 antigens and EBOV GP was performed to determine the stability of GP expression from all vectors. All seed pool clones were initially screened, and those with 100% GP expression were selected for preparation of working pools, which were also analyzed by double staining to ensure no loss of GP expression. Briefly, Vero cells were infected with a 10-fold serially diluted inoculum and incubated for 6 days at 32°C under a 0.8% methylcellulose overlay Opti-MEM I medium containing 4% trypsin. For samples derived from African green monkeys, ampicillin (200 μg/ml), cleocin (30 μg/ml), timentin (400 μg/ml), gentamicin (100 μg/ml), and amphotericin (5 μg/ml) were included in the overlay medium. At 6 days postinfection, cells were fixed twice with ice-cold 80% methanol. Immunostaining was performed with an HPIV1-specific goat polyclonal antibody (ab20791; Abcam, Cambridge, MA) and a mouse monoclonal EBOV GP antibody (4F3; IBT Bioservices, Rockville, MD) at dilutions of 1:1,600 and 1:2,000, respectively. The secondary antibodies were infrared dye-conjugated donkey anti-goat immunoglobulin 680LT and donkey anti-mouse immunoglobulin 800CW (Li-Cor, Lincoln, NE), each used at a 1:800 dilution. Images were acquired using an Odyssey infrared imaging system. Plaques were pseudocolored to appear red and green for HPIV1 and EBOV GP expression, respectively. HPIV1 plaques expressing EBOV GP appeared yellow (HPIV1 and GP staining merged).

Double-staining flow cytometry assay. The small plaque sizes of the GP-TMCT1 and GP-TMCT2 constructs impeded assessment of GP stability by plaque staining, and therefore, a flow cytometry-based assay was developed. Briefly, Vero cells infected at an MOI of 5 $TCID_{50}$ per cell were harvested at 24 h p.i. with 1 mM EDTA in phosphate-buffered saline (PBS). Cells were first stained with LIVE/DEAD fixable near-infrared amine-reactive dead cell discriminating dye (Life Technologies) followed by HPIV1

F-specific mouse monoclonal antibody (clone 7.1 at a 1:1,000 dilution pretitrated to achieve specific F detection with no detectable background staining) and anti-EBOV GP human monoclonal antibody (KZ52 at a 1:300 dilution; IBT Bioservices). Cells were washed and stained with the secondary goat anti-mouse Alexa Fluor 647 and goat anti-human Alexa Fluor 488 (Life Technologies) antibodies. All antibody dilutions and washes were performed with FACS buffer (PBS containing 2% FBS). Cells were fixed and data were acquired on BD FACSCanto II and analyzed using FlowJo, version 10.1 (Ashland, OR). Cells were sequentially gated on forward scatter (FSC) versus side scatter (SSC), single cells, live cells, HPIV1 F^+ cells, and finally GP^+ cells. An average total of 15,000 HPIV1 F^+ cells were evaluated to determine the percentage of GP^+ cells.

Western blot analysis: GP expression in infected cells and incorporation in the rHPIV1 particles. Vero cells were infected at an MOI of 3 $TCID_{50}$ with the four constructs, including wt HPIV1 and HPIV1-$C^{\Delta 170}$ empty vector as controls, and incubated at 32°C for 48 h. Cell lysates were prepared by direct lysis of the monolayer with 100 μl of 1× lithium dodecyl sulfate (LDS) sample buffer, and 22.5 μl of lysate was reduced, denatured, and electrophoresed on a 4 to 12% bis-Tris SDS gel (Life Technologies). Proteins were transferred to a polyvinylidene difluoride (PVDF) membrane and analyzed by Western blotting.

To analyze EBOV GP incorporation in the HPIV1 vector virions, LLC-MK2 cells were infected at an MOI of 0.1 $TCID_{50}$ per cell with viruses expressing EBOV GP, wt HPIV1, and rHPIV1-$C^{\Delta 170}$ empty vector and incubated at 32°C for 6 days. The medium supernatant was clarified, and virus was purified by discontinuous sucrose gradient centrifugation. The protein content of each purified virus was determined by bicinchoninic acid (BCA) assay (Thermo Fisher Scientific). One microgram of protein of each sucrose-purified virus preparation was lysed in radioimmunoprecipitation assay (RIPA) buffer and subjected to SDS-PAGE and Western blot analysis.

NHP studies. All animal studies were approved by the National Institutes of Health (NIH) Institutional Animal Care and Use Committee (IACUC). *In vivo* replication and immunogenicity were assessed in AGMs. Animals were confirmed to be naive for HPIV1 and HPIV3 by serum hemagglutination inhibition assay (35), and four animals per virus were infected by the combined i.n. and intratracheal (i.t.) routes with 10^6 $TCID_{50}$ per site, in parallel with two animals infected with wt HPIV1 for comparison. The previously described candidate rHPIV3/EboGP (21) was also included with two animals as a positive reference. Nasopharyngeal (NP) swabs were collected daily for 14 days, whereas tracheal lavage (TL) with 3 ml of PBS was performed every other day p.i. for 14 days. After 28 days two animals of each group received a second inoculation (boost) with the same virus. Dose, routes, and NP/TL sample collection were the same as for the first dose. Virus titers of NP and TL samples were determined by serial dilution on LLC-MK2 cells and HAD assay and reported as $\log_{10}$ $TCID_{50}$ per milliliter. For each virus, NP and TL samples from 4 animals at their peak titer day following the first inoculation as well as a day before and after were subjected to double-staining plaque assay to determine the stability of GP expression during *in vivo* replication. Serum was collected from all animals weekly, starting on the day of inoculation, to determine GP-specific antibody response following the first and second doses.

EBOV GP-specific IgG ELISA. A commercially available monkey anti-Zaire EBOV GP IgG ELISA kit (Alpha Diagnostic International Inc., San Antonio, TX) was used to quantify the GP-specific serum antibody response of the immunized AGMs. The assay was performed as described in the manufacturer's protocol. Briefly, 5-fold serially diluted serum was added to EBOV-GP-coated wells of a 96-well ELISA plate and incubated for 1 h to capture GP-specific antibodies. The wells were washed and the bound GP antibodies were detected with a secondary horseradish peroxidase-conjugated anti-monkey IgG. The absorbance at 450 nm was measured, and the dilution of each sample yielding a value of 1 for optical density at 450 nm (OD_{450}) was calculated by linear regression analysis.

EBOV GP neutralization assay. Serum titers of EBOV GP-specific neutralizing antibodies were determined by a 60% plaque reduction neutralization test ($PRNT_{60}$) on Vero cells using a HPIV3-based construct (called rHPIV3/NotI ΔF-HN/EboGP) that lacks the HPIV3 F and HN glycoprotein genes and expresses the EBOV GP from an added gene as the sole viral surface protein. This virus is very similar to another version reported previously (20). Sera were heated at 56°C for 30 min, and 4-fold serial dilutions were made. These were combined with a set amount of virus and adjusted to contain 10% (vol/vol) of a commercial preparation of guinea pig complement (Lonza, Allendale, NJ), incubated for 30 min at 37°C, and then transferred to Vero cell monolayers in 24-well plates. As a positive control, the human monoclonal antibody KZ52 (IBT Bioservices), which is a purified antibody preparation, was included at 1.49 mg/ml. It is an EBOV GP-specific monoclonal antibody derived from an EBOV survivor and has been shown to neutralize EBOV to 50% at 0.3 μg/ml (36). Inoculated cells were rocked for 2 h at 32°C on a rocking platform, overlaid with Opti-MEM I medium (containing 0.8% methylcellulose, 2% FBS, 1× L-glutamine, and 50 μg/ml of gentamicin), and incubated for 6 days at 32°C. The cells were fixed twice with ice-cold 80% methanol, and plaques were detected with mouse anti-GP antibody and a secondary goat anti-mouse infrared-conjugated 680RD antibody. $PRNT_{60}$ titer was calculated by linear regression analysis. To confirm that HPIV1- or HPIV3-specific antibodies present in the samples did not neutralize the rHPIV3/NotI ΔF-HN/EboGP virus, control HPIV1 and HPIV3 hyperimmune rabbit sera, with known, high HPIV1 or HPIV3 neutralization titers, were included as controls that showed no detectable neutralizing activity, indicating that neutralization was specific to anti-EBOV GP antibodies.

ACKNOWLEDGMENTS

This research was supported by the Intramural Research Program of the NIAID, NIH.

We thank Joanna Swerczek from the Experimental Primate Virology Section, Comparative Medicine Branch, NIAID, NIH, Poolesville, MD, for technical assistance during

AGM experiments and for the care and management of animals. We also thank Mario Skiadopoulos and Brian R. Murphy for providing the antipeptide antisera against the HPIV1 N, P, F, and HN proteins.

REFERENCES

1. Misasi J, Sullivan NJ. 2014. Camouflage and misdirection: the full-on assault of Ebola virus disease. Cell 159:477–486. https://doi.org/10.1016/j.cell.2014.10.006.
2. Kuhn JH, Dodd LE, Wahl-Jensen V, Radoshitzky SR, Bavari S, Jahrling PB. 2011. Evaluation of perceived threat differences posed by filovirus variants. Biosecur Bioterror 9:361–371. https://doi.org/10.1089/bsp.2011.0051.
3. CDC. 14 April 2016. Ebola outbreak in West Africa—case counts. https://www.cdc.gov/vhf/ebola/outbreaks/2014-west-africa/case-counts.html. Accessed 12 September 2016.
4. Osterholm MT, Moore KA, Kelley NS, Brosseau LM, Wong G, Murphy FA, Peters CJ, LeDuc JW, Russell PK, Van Herp M, Kapetshi J, Muyembe JJ, Ilunga BK, Strong JE, Grolla A, Wolz A, Kargbo B, Kargbo DK, Sanders DA, Kobinger GP. 2015. Transmission of Ebola viruses: what we know and what we do not know. mBio 6:e00137. https://doi.org/10.1128/mBio.00137-15.
5. Johnson E, Jaax N, White J, Jahrling P. 1995. Lethal experimental infections of rhesus monkeys by aerosolized Ebola virus. Int J Exp Pathol 76:227–236.
6. Jaax N, Jahrling P, Geisbert T, Geisbert J, Steele K, McKee K, Nagley D, Johnson E, Jaax G, Peters C. 1995. Transmission of Ebola virus (Zaire strain) to uninfected control monkeys in a biocontainment laboratory. Lancet 346:1669–1671. https://doi.org/10.1016/S0140-6736(95)92841-3.
7. Wong G, Qiu X, Richardson JS, Cutts T, Collignon B, Gren J, Aviles J, Embury-Hyatt C, Kobinger GP. 2015. Ebola virus transmission in guinea pigs. J Virol 89:1314–1323. https://doi.org/10.1128/JVI.02836-14.
8. Sanchez A, Trappier SG, Mahy BW, Peters CJ, Nichol ST. 1996. The virion glycoproteins of Ebola viruses are encoded in two reading frames and are expressed through transcriptional editing. Proc Natl Acad Sci U S A 93:3602–3607. https://doi.org/10.1073/pnas.93.8.3602.
9. Bukreyev A, Rollin PE, Tate MK, Yang L, Zaki SR, Shieh WJ, Murphy BR, Collins PL, Sanchez A. 2007. Successful topical respiratory tract immunization of primates against Ebola virus. J Virol 81:6379–6388. https://doi.org/10.1128/JVI.00105-07.
10. Meyer M, Garron T, Lubaki NM, Mire CE, Fenton KA, Klages C, Olinger GG, Geisbert TW, Collins PL, Bukreyev A. 2015. Aerosolized Ebola vaccine protects primates and elicits lung-resident T cell responses. J Clin Invest 125:3241–3255. https://doi.org/10.1172/JCI81532.
11. Mire CE, Matassov D, Geisbert JB, Latham TE, Agans KN, Xu R, Ota-Setlik A, Egan MA, Fenton KA, Clarke DK, Eldridge JH, Geisbert TW. 2015. Single-dose attenuated Vesiculovax vaccines protect primates against Ebola Makona virus. Nature 520:688–691.
12. Stanley DA, Honko AN, Asiedu C, Trefry JC, Lau-Kilby AW, Johnson JC, Hensley L, Ammendola V, Abbate A, Grazioli F, Foulds KE, Cheng C, Wang L, Donaldson MM, Colloca S, Folgori A, Roederer M, Nabel GJ, Mascola J, Nicosia A, Cortese R, Koup RA, Sullivan NJ. 2014. Chimpanzee adenovirus vaccine generates acute and durable protective immunity against ebolavirus challenge. Nat Med 20:1126–1129.
13. Ewer K, Rampling T, Venkatraman N, Bowyer G, Wright D, Lambe T, Imoukhuede EB, Payne R, Fehling SK, Strecker T, Biedenkopf N, Krahling V, Tully CM, Edwards NJ, Bentley EM, Samuel D, Labbe G, Jin J, Gibani M, Minhinnick A, Wilkie M, Poulton I, Lella N, Roberts R, Hartnell F, Bliss C, Sierra-Davidson K, Powlson J, Berrie E, Tedder R, Roman F, De Ryck I, Nicosia A, Sullivan NJ, Stanley DA, Mbaya OT, Ledgerwood JE, Schwartz RM, Siani L, Colloca S, Folgori A, Di Marco S, Cortese R, Wright E, Becker S, Graham BS, Koup RA, Levine MM, Volkmann A, Chaplin P, Pollard AJ, Draper SJ, Ballou WR, Lawrie A, Gilbert SC, Hill AV. 2016. A monovalent chimpanzee adenovirus Ebola vaccine boosted with MVA. N Engl J Med 374:1635–1646. https://doi.org/10.1056/NEJMoa1411627.
14. Karron RA, Buchholz UJ, Collins PL. 2013. Live-attenuated respiratory syncytial virus vaccines. Curr Top Microbiol Immunol 372:259–284.
15. Bartlett EJ, Cruz AM, Esker J, Castano A, Schomacker H, Surman SR, Hennessey M, Boonyaratanakornkit J, Pickles RJ, Collins PL, Murphy BR, Schmidt AC. 2008. Human parainfluenza virus type 1 C proteins are nonessential proteins that inhibit the host interferon and apoptotic responses and are required for efficient replication in nonhuman primates. J Virol 82:8965–8977. https://doi.org/10.1128/JVI.00853-08.
16. Bartlett EJ, Castano A, Surman SR, Collins PL, Skiadopoulos MH, Murphy BR. 2007. Attenuation and efficacy of human parainfluenza virus type 1 (HPIV1) vaccine candidates containing stabilized mutations in the P/C and L genes. Virol J 4:67. https://doi.org/10.1186/1743-422X-4-67.
17. Mackow N, Amaro-Carambot E, Liang B, Surman S, Lingemann M, Yang L, Collins PL, Munir S. 2015. Attenuated human parainfluenza virus type 1 (HPIV1) expressing the fusion glycoprotein of human respiratory syncytial virus (RSV) as a bivalent HPIV1/RSV vaccine. J Virol 89:10319–10332. https://doi.org/10.1128/JVI.01380-15.
18. Bartlett EJ, Amaro-Carambot E, Surman SR, Collins PL, Murphy BR, Skiadopoulos MH. 2006. Introducing point and deletion mutations into the P/C gene of human parainfluenza virus type 1 (HPIV1) by reverse genetics generates attenuated and efficacious vaccine candidates. Vaccine 24:2674–2684. https://doi.org/10.1016/j.vaccine.2005.10.047.
19. Newman JT, Riggs JM, Surman SR, McAuliffe JM, Mulaikal TA, Collins PL, Murphy BR, Skiadopoulos MH. 2004. Generation of recombinant human parainfluenza virus type 1 vaccine candidates by importation of temperature-sensitive and attenuating mutations from heterologous paramyxoviruses. J Virol 78:2017–2028. https://doi.org/10.1128/JVI.78.4.2017-2028.2004.
20. Bukreyev A, Marzi A, Feldmann F, Zhang L, Yang L, Ward JM, Dorward DW, Pickles RJ, Murphy BR, Feldmann H, Collins PL. 2009. Chimeric human parainfluenza virus bearing the Ebola virus glycoprotein as the sole surface protein is immunogenic and highly protective against Ebola virus challenge. Virology 383:348–361. https://doi.org/10.1016/j.virol.2008.09.030.
21. Bukreyev A, Yang L, Zaki SR, Shieh WJ, Rollin PE, Murphy BR, Collins PL, Sanchez A. 2006. A single intranasal inoculation with a paramyxovirus-vectored vaccine protects guinea pigs against a lethal-dose Ebola virus challenge. J Virol 80:2267–2279. https://doi.org/10.1128/JVI.80.5.2267-2279.2006.
22. Kapikian AZ, Chanock RM, Reichelderfer TE, Ward TG, Huebner RJ, Bell JA. 1961. Inoculation of human volunteers with parainfluenza virus type 3. JAMA 178:537–541.
23. Liang B, Ngwuta JO, Herbert R, Swerczek J, Dorward DW, Amaro-Carambot E, Mackow N, Kabatova B, Lingemann M, Surman S, Yang L, Chen M, Moin SM, Kumar A, McLellan JS, Kwong PD, Graham BS, Schaap-Nutt A, Collins PL, Munir S. 14 September 2016. Packaging and prefusion stabilization separately and additively increase the quantity and quality of RSV-neutralizing antibodies induced by respiratory syncytial virus (RSV) fusion protein expressed by a parainfluenza vector. J Virol https://doi.org/10.1128/JVI.01196-16.
24. Bachmann MF, Rohrer UH, Kundig TM, Burki K, Hengartner H, Zinkernagel RM. 1993. The influence of antigen organization on B cell responsiveness. Science 262:1448–1451.
25. Durbin AP, Elkins WR, Murphy BR. 2000. African green monkeys provide a useful nonhuman primate model for the study of human parainfluenza virus types-1, -2, and -3 infection. Vaccine 18:2462–2469. https://doi.org/10.1016/S0264-410X(99)00575-7.
26. Yang CF, Wang CK, Malkin E, Schickli JH, Shambaugh C, Zuo F, Galinski MS, Dubovsky F, Study Group, Tang RS. 2013. Implication of respiratory syncytial virus (RSV) F transgene sequence heterogeneity observed in Phase 1 evaluation of MEDI-534, a live attenuated parainfluenza type 3 vectored RSV vaccine. Vaccine 31:2822–2827. https://doi.org/10.1016/j.vaccine.2013.04.006.
27. Bukreyev AA, Dinapoli JM, Yang L, Murphy BR, Collins PL. 2010. Mucosal parainfluenza virus-vectored vaccine against Ebola virus replicates in the respiratory tract of vector-immune monkeys and is immunogenic. Virology 399:290–298. https://doi.org/10.1016/j.virol.2010.01.015.
28. Medina MF, Kobinger GP, Rux J, Gasmi M, Looney DJ, Bates P, Wilson JM. 2003. Lentiviral vectors pseudotyped with minimal filovirus envelopes increased gene transfer in murine lung. Mol Ther 8:777–789. https://doi.org/10.1016/j.ymthe.2003.07.003.
29. Connors M, Collins PL, Firestone CY, Sotnikov AV, Waitze A, Davis AR,

Hung PP, Chanock RM, Murphy BR. 1992. Cotton rats previously immunized with a chimeric RSV FG glycoprotein develop enhanced pulmonary pathology when infected with RSV, a phenomenon not encountered following immunization with vaccinia-RSV recombinants or RSV. Vaccine 10:475–484.
30. Buchholz UJ, Finke S, Conzelmann KK. 1999. Generation of bovine respiratory syncytial virus (BRSV) from cDNA: BRSV NS2 is not essential for virus replication in tissue culture, and the human RSV leader region acts as a functional BRSV genome promoter. J Virol 73:251–259.
31. Volchkov VE, Volchkova VA, Muhlberger E, Kolesnikova LV, Weik M, Dolnik O, Klenk HD. 2001. Recovery of infectious Ebola virus from complementary DNA: RNA editing of the GP gene and viral cytotoxicity. Science 291:1965–1969. https://doi.org/10.1126/science.1057269.
32. Kolakofsky D, Pelet T, Garcin D, Hausmann S, Curran J, Roux L. 1998. Paramyxovirus RNA synthesis and the requirement for hexamer genome length: the rule of six revisited. J Virol 72:891–899.
33. Bartlett EJ, Amaro-Carambot E, Surman SR, Newman JT, Collins PL, Murphy BR, Skiadopoulos MH. 2005. Human parainfluenza virus type I (HPIV1) vaccine candidates designed by reverse genetics are attenuated and efficacious in African green monkeys. Vaccine 23:4631–4646. https://doi.org/10.1016/j.vaccine.2005.04.035.
34. Newman JT, Surman SR, Riggs JM, Hansen CT, Collins PL, Murphy BR, Skiadopoulos MH. 2002. Sequence analysis of the Washington/1964 strain of human parainfluenza virus type 1 (HPIV1) and recovery and characterization of wild-type recombinant HPIV1 produced by reverse genetics. Virus Genes 24:77–92. https://doi.org/10.1023/A:1014042221888.
35. van Wyke Coelingh KL, Winter CC, Tierney EL, London WT, Murphy BR. 1988. Attenuation of bovine parainfluenza virus type 3 in nonhuman primates and its ability to confer immunity to human parainfluenza virus type 3 challenge. J Infect Dis 157:655–662.
36. Maruyama T, Rodriguez LL, Jahrling PB, Sanchez A, Khan AS, Nichol ST, Peters CJ, Parren PW, Burton DR. 1999. Ebola virus can be effectively neutralized by antibody produced in natural human infection. J Virol 73:6024–6030.